

Passivation of the calcite surface with malonate ion

Manlio F. Salinas-Nolasco,^a Juan Méndez-Vivar,^{a,*} Víctor H. Lara,^a and Pedro Bosch^b

^a *Universidad Autónoma Metropolitana Iztapalapa, Departamento de Química, A.P. 55-534, México D.F. 09340, Mexico*

^b *Instituto de Investigación en Materiales, Universidad Nacional Autónoma de México, Circuito Interior, Ciudad Universitaria, México D.F. 4510, Mexico*

Received 4 August 2003; accepted 23 October 2003

Abstract

Samples of polycrystalline calcite were impregnated with solutions of malonic acid of three concentrations (5×10^{-2} , 5×10^{-3} , and 5×10^{-4} M) and different pH values (6.00, 7.00, and 8.00). The impregnation was carried out at room temperature to evaluate the adsorption of malonate ion in the calcite surface to optimize the conditions for possible application on limestone and marble in cultural heritage materials. The affinity of the malonate ion was determined through the potentiometric measurement of the surface charge and the corresponding adsorbed amounts by titration, Raman spectroscopy, and small-angle X-ray scattering (SAXS). The results indicate effective adsorption of the malonate ion on the surface at a pH value close to the point of zero charge ($\text{pH}_{\text{pzc}} \approx 8.20$) and changes in some surface morphological properties such as the pore shape and the pore size distribution. The presence of a malonate adsorptive layer on calcite generates an interface interaction potential that may influence the reaction and transport mechanisms within the medium.

© 2003 Elsevier Inc. All rights reserved.

Keywords: Calcium carbonate; Calcite; Malonate ion; Passivation; Surface charge; Raman spectroscopy; SAXS

1. Introduction

The study of calcium carbonate surface properties is very important in order to understand biochemical and geological phenomena. These include precipitation, crystal growth and dissolution, and even the formation of rigid structures [1–5]. The understanding of processes that occur on calcium carbonate surfaces plays an important role in several fields, e.g., the conservation of cultural heritage materials built from marble and limestone. In order to prevent the deterioration of these cultural objects it is important to search for new compounds that accomplish several requirements: to keep the original appearance of the objects and to be gentle to the surface, among others.

The passivation of calcium carbonate consists of chemical adsorption of small molecules, generally organics, which protect the object in a nonpermanent and nonaggressive way, without modifying the surface structural properties [6,7], which are important for the natural dynamical processes in the stone. Moreover, the presence of a chemical agent on the surface influences mass and energy transport mecha-

nisms, inhibits surface dissolution, and avoids morphology changes.

According to the literature, calcium carbonate exhibits chemical affinity with several organic compounds, particularly if these have polar functional groups [8,9]. The natural organic polyelectrolytes are effective crystal growth inhibitors of calcium carbonate, and there are computational models to evaluate the chemical potential of such substances acting as inhibitors [10]. In addition, organic and inorganic additives play an important role in crystallization processes. Extensive studies of several additives and their effects have been performed recently [11–13]. In those cases, however, the main studied phenomenon was surface complexation in aqueous solutions, which promoted the multilayer formation of adsorbate on the surface [14–17].

Ca^{2+} is a highly reactive ion in complex formation. Complex formation with polyelectrolytes requires chelating molecules as a necessary condition, as well as the ability to form chelating rings. The high calcium coordination number, ranging from 3 up to 10, results in a large electrophilic power. The evidence of dicarboxylic acid affinity with calcium carbonate started with studies of maleic and fumaric [18], tartaric [19], and polymaleic acids [20]. Later on, a study with α , ω -dicarboxylates [21] showed the

* Corresponding author.

E-mail address: jmv@xanum.uam.mx (J. Méndez-Vivar).

strong affinity of malonic acid compared to other dicarboxylic acids. Hence the molecular structure and the number of carbon atoms in the main chain are important factors in preferential adsorption on calcium carbonate. Recent studies have demonstrated the ability of malonic acids to modify the crystallization habit [22], to lower the rate of crystal growth [23], and to generate surface complexation on calcite in water [24]. The goal of this work was to use malonic acid solutions to passivate the calcite surface. The morphological alterations found were correlated with pH and surface polarizability. According to the results, the malonate ion modifies the pore shape, pore size distribution, and surface electronic density.

2. Experimental

The malonic acid used was an analytical reagent from Sigma–Aldrich Co., and it was used without further purification. Deionized water (conductivity < 18 mS) was used to prepare all solutions. Three malonate ion solutions were prepared: 5×10^{-2} , 5×10^{-3} , and 5×10^{-4} M. The pH of malonic acid solutions were adjusted to 6.00, 7.00, and 8.00 by addition of 1.6 M NH_4OH (Baker), which had previously been standardized with dihydrated oxalic acid (Sigma–Aldrich) to 0.4 M concentration. The pH control and variations in time were registered using a Conductronic PC43 potentiometer, PC100C-BNC epoxy body electrode (± 0.01 pH). The potentiometer was calibrated with buffer solutions (Sigma–Aldrich) at pH values 4.00, 7.00, and 10.00.

The calcium carbonate was a polycrystalline precipitate of marble powder from Conservator's Emporium (Reno, Nevada, USA), highly pure, with average particle diameter 2.70 ± 0.60 μm , consisting in crystalline calcite, as confirmed by X-ray diffraction (XRD) and infrared spectroscopy (FTIR) analyses.

The calcite impregnations were done by dispersing 5.0 g of calcium carbonate into 50.0 ml of the malonic acid solutions, using a high-speed stirrer, enough to keep the suspensions homogenized for 4 h at room temperature (293 K). The suspensions were allowed to sediment by gravity for 72 h. The sediment was then decanted and filtered by gravity in a Whatman 41 paper filter. The powder was washed with 40.0 ml of deionized water. The solid was dried for 48 h at 353 K. The dry sample was collected as a fine powder for subsequent analysis.

FTIR spectroscopy measurements were performed in Perkin–Elmer 16PC equipment at room temperature (293 K) in air. Conventional X-ray diffractograms were obtained with a Siemens D500 diffractometer coupled to a Cu anode tube. The $K\alpha$ radiation was selected with a diffracted beam monochromator. Raman spectroscopy measurements were performed at room temperature in air with a Spex 1403 double monochromator using the 514.5-nm line of an argon (Laser Ionics) laser at a power level of 150 mW in a quasi-

backscattering configuration. The signal was detected with a photomultiplier and a standard photon-counting system. The small angle X-ray scattering (SAXS) curves ($I(h)$ vs h , where $I(h)$ is the intensity and $h = 4\pi \sin \theta / \lambda$, with λ as the wavelength and θ the scattering angle) were measured using a Kratky camera coupled to a Cu anode tube and a Ni filter. The data, collected with a proportional linear counter, were the input of the program ITP [25–28]. From the Kratky plots the shape of the heterogeneities in the samples was determined [29].

3. Results

The marble powder used is a polycrystalline solid of calcite crystallographic unitary cell. The common preferential cleavage plane is (1 0 | 4). This was verified by X-ray diffraction (XRD) and corresponds to a rhombohedral surface [30]. The surface area resulting from BET nitrogen adsorption was 2.70 m^2/g , compared to 0.40 m^2/g for a monocystal. The dimensions of the unitary cell reported are $5.0 \times 8.1 \text{ \AA}$ [31] and the number of basic sites is 5.0 site/ nm^2 [16]. The sample has an average pore radius of 102 \AA , consisting of a mixture of micro and mesopores.

Ionic minerals such as calcite present complex mechanisms in aqueous solutions. The surface charge (σ) in calcite dissolution depends on two mechanisms: (a) adsorption of water molecules (dipoles) on H^+ or OH^- ions onto the solid surface followed by the dissociation of the hydrolytic product formed and (b) preferential release of some lattice ion species from the solid phase as a result of different hydration energies and readsorption of hydrolytic lattice products. The calcite ions (including Ca^{2+} and CO_3^{2-}) are potential-determining ions (PDI), though the preferential hydrolysis of surface ions or electrolyte adsorption by complex formation in solution can establish the surface charge. The pH oscillation shows a succession of fast and slow reactions to establish the surface charge during the calcite aqueous dissolution. This mechanism plays an important role in pH regulation in marine environments [16]. The elementary and simplified proposal of Akin and Lagerwerff [32] suggested that H^+ and OH^- are the potential-determining ions across the reactions:



The surface charge is defined by

$$\sigma = F(\Gamma_{\text{H}^+} - \Gamma_{\text{OH}^-}), \quad (3)$$

where σ is the surface charge in C/m^2 , F is the Faraday constant, and Γ_{H^+} and Γ_{OH^-} are adsorption densities of H^+ and OH^- in mol/m^2 . The surface charge σ can be calculated from the change of pH value in an aqueous suspension of the solid. The first adsorption step is fast and may be finished in a few minutes; the second step is slow and the equilibrium is reached in several hours.

The complete description of the potential-determining ions in calcite dissolution considers all present and susceptible ions to be adsorbed [16]. The surface speciation analysis has shown that a combinatorial set of chemical equilibria for surface reactions can exist and it is possible to determine the ionic species predominance diagrams for the calcite surface as a pH function. The generalized surface charge can be determined,

$$\sigma = Fk^* \sum a[M]_i, \quad (4)$$

where $[M]_i$ is the molarity of the ionic species adsorbed on the calcite surface, $k^* = V/Sm$, V is the suspension volume, S is the surface area, m is the calcium carbonate sample mass, and the a value is +1 for cations and -1 for anions. Comparing Eqs. (3) and (4), it is possible to establish the electroneutrality principle for the calcite dissolution in the equilibrium state:

$$[H^+] - [OH^-] = [CO_3^{2-}] + [HCO_3^-] - [Ca^{2+}] - [CaOH^+] - [CaHCO_3^+]. \quad (5)$$

As a first approximation, it is possible to calculate the surface charge from the difference between initial and final pH values. The presence of additive malonate ions in the solution modifies the charge balance in the electroneutrality of chemical equilibrium:

$$[H^+] - [OH^-] = [CO_3^{2-}] + [HCO_3^-] - [Ca^{2+}] - [CaOH^+] - [CaHCO_3^+] + [HMal^-] + [Mal^{2-}]. \quad (6)$$

The calculation of the surface charge using Eq. (3) is equivalent to considering all the ions of surface speciation [33].

3.1. Isoelectric point and point of zero charge

Fig. 1 shows the surface charge values in an aqueous calcite solution as a function of pH, obtained using Eq. (3), in chemical equilibrium at room temperature. It is important to point out that (a) a minimum surface charge value

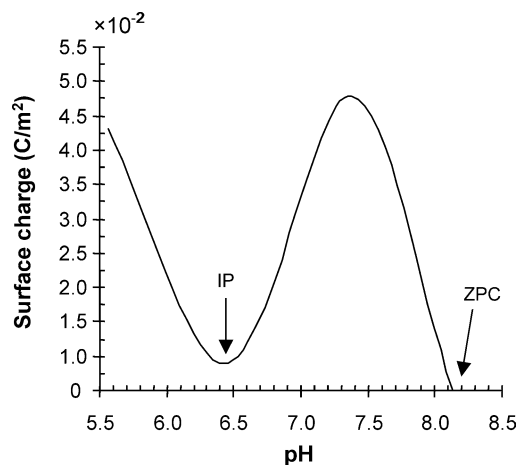


Fig. 1. Surface charge of calcite in aqueous solution at room temperature, calculated using Eq. (3).

point appears at pH 6.45, (b) a maximum point appears at pH 7.38, and (c) a zero value appears at pH 8.2. The last is known as the point of zero charge (PZC), as the concentration of potential-determining ions for a surface charge of calcite $\sigma = 0$. The point (a) is called the isoelectric point (IP) as the concentration of potential-determining ions at which the electrokinetic zeta potential $\zeta = 0$ [34]. According to the IUPAC, PZC refers to a particle or surface carrying no fixed charge and IP to a particle showing no electrophoreses or a surface showing no electroosmosis. The calcite solution in the IP has a surface charge, but there is no ionic mobility. This condition is considered as a metastable equilibrium that allows chemical interactions [35].

Previous studies indicate that the IP of calcite occurs at $pH > 5.5$ and PZC at pH 8.2. These values depend on the solution composition [31], and if the system is open or closed. The record of these values is reported as an interval. Between the IP and PZC it is possible to encounter the main mechanisms of reactivity and speciation, because this range determines the mobility and the surface charge composition due to the ionic species present. Thus, it is necessary to promote surface complexation with malonate ion between the values of IP and PZC [33].

3.2. Malonic acid solutions

The predominance diagram of the ionic species derived from malonic acid (which is a weak organic acid) as a pH function is presented in Fig. 2, which shows that totally dissociated chemical species exist at $pH > 5.90$. Considering that these species are more susceptible to an effective interaction, besides the negative partial charge in the extreme functional group (see Fig. 3), the useful experimental pH interval in the complexation of calcite should be the one including $pH > pK_2$, the IP and the PZC pH values. In addition,

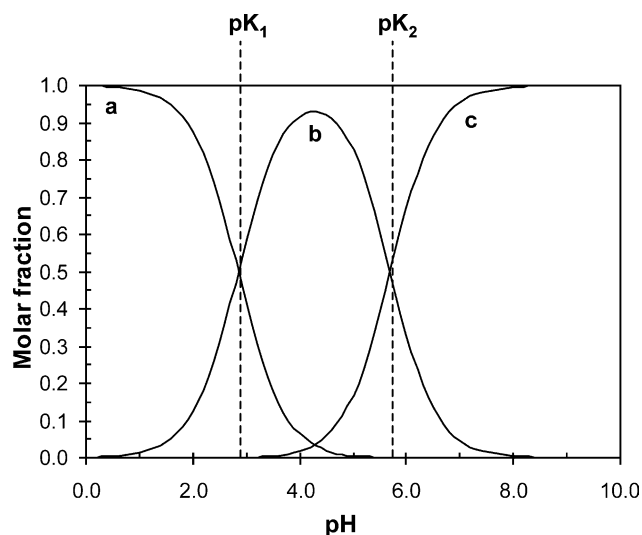


Fig. 2. Generalized predominance diagram of chemical species derived from malonic acid: (a) nondissociated species; (b) monodissociated species; and (c) malonate ion.

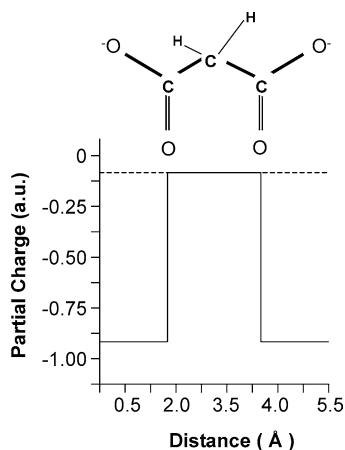


Fig. 3. Partial charge values of malonic acid calculated by the Sanderson equalization principle [36].

tion, it is relevant to mention the importance of stereochemical configuration of dicarboxylic acid in the effective adsorption on calcite. The correlation of a topological parameter (i.e., the Randic index [37]) with some properties of the dicarboxylic acid shows that the molecular structure correlates adequately to the physicochemical properties. Regarding the surface affinity of dicarboxylic acids to calcite, the work of Mann et al. [21] is an excellent example of this criterion: the adsorption ability depends on the carbon number between the carboxylate functional groups of the molecule. According to those results, malonic acid is the best dicarboxylic acid for adsorption on calcite in aqueous media.

3.3. Surface charge

Table 1 shows the dependence of the surface charge on pH for three concentrations. These values of σ are smaller than those obtained for pure calcite. In all cases, the impregnation resulted in a diminution of the surface charge. The pH closer to the PZC favors a significant diminution of surface charge, compared to the corresponding pH value close to IP. The electroneutrality of the calcite surface, defined by PZC, is a main condition for a chemical equilibrium independent of the concentration. In the intermediate interval, the surface charge acquires the lowest value, probably due to the adsorption mechanisms between two limit states.

The electrostatic nature of the malonic acid adsorption was demonstrated during washing of the samples with deionized water. Table 2 shows the surface charge after washing for the various pH values of the impregnation. The surface charge, in all cases, increased by two magnitude orders. However, these values are smaller than the calcite surface charge without impregnation. Therefore the malonate ion layer under the rigid transport conditions of mixing accounts for an important amount. The lower surface charge is reached at a lower pH values and higher concentrations. The pH value closer to IP has a smaller charge than the value for impregnation, whose charge is smaller than PZC. Therefore, the pH values closer to IP are favorable to increasing

Table 1
Surface charge of the calcite samples by impregnation at three concentrations of malonic acid solutions

Concentration	pH _{exp} ^a	pH _{eq} ^b	$\sigma_{\text{calcite}}/10^{-4}$ (C/m ²) ^c
5×10^{-2} M	6.00	7.72	1.67
	7.00	7.97	-2.66
	8.00	8.25	-2.77
5×10^{-3} M	6.00	8.06	-0.52
	7.00	8.33	-6.94
	8.00	8.40	-5.38
5×10^{-4} M	6.00	8.02	-0.17
	7.00	7.96	-2.58
	8.00	8.23	-2.48

^a pH at initial experimental condition of impregnation (± 0.01).

^b pH at final experimental condition in equilibrium after 48 h of impregnation (± 0.02).

^c Surface charge calculated by Eq. (3) for $V = 50.0$ ml, $S = 2.7$ m²/g, and $m = 5.0$ g.

Table 2
Surface charge of the calcite samples impregnated with malonic acid solutions after washing with deionized water (pH 7.17 ± 0.1)

Concentration	pH _{exp} ^a	pH _{eq} ^b	$\sigma_{\text{calcite}}/10^{-4}$ (C/m ²) ^c
5×10^{-2} M	6.00	8.44	-113.57
	7.00	8.57	-156.46
	8.00	8.61	-172.46
5×10^{-3} M	6.00	8.38	-97.71
	7.00	8.47	-122.35
	8.00	8.58	-160.32
5×10^{-4} M	6.00	8.26	-71.90
	7.00	8.41	-105.37
	8.00	8.39	-100.21

^a pH at initial experimental condition of impregnation (± 0.01).

^b pH at final experimental condition in equilibrium after 48 h of washing (± 0.018).

^c Surface charge calculated by Eq. (3) for $V = 50.0$ ml, $S = 2.7$ m²/g, and $m = 0.4 \pm 0.1$ g.

the adsorption. Regarding to the concentration, 5×10^{-2} M is, then, the most adequate concentration for adsorption.

3.4. Adsorbed malonic acid

The amounts of malonic acid adsorbed on the calcite surface were calculated considering the initial equilibrium of the malonic acid solutions at the experimental pH value,

$$[\text{H}^+] = [\text{OH}^-] + [\text{HMal}^-] + [\text{Mal}^{2-}], \quad (7)$$

and the final equilibrium of the impregnation solution, stated by Eq. (6). The concentration of adsorbed malonic acid $[\text{AcMal}]_{\text{ads}}$ as the molarity is the difference between the initial experimental concentration and the final equilibrium concentration. We did not consider other chemical associations, such as those occurring between NH_4^+ and CO_3^{2-} (NH_4CO_3^-), or Ca^{2+} and HMal^- (CaHMal^+); such chemical species are considered ampholytes, whose insta-

Table 3

Adsorbed amounts (Γ_{AcMal}), relative adsorption amounts (K_{ads}), and adsorbed sites on calcite surface by impregnation with malonic acid solutions

Concentration	pH _{exp} ^a	Γ_{AcMal} ($\mu\text{mol}/\text{m}^2$) ^b	K_{ads} ^c	$\text{p}K_{\text{ads}}$ ^d	Adsorbed sites (molec/site) ^e
5×10^{-2} M	6.00	7.9739	23.22	-1.37	0.96
	7.00	8.2253	22.54	-1.35	0.99
	8.00	8.9739	20.64	-1.31	1.08
5×10^{-3} M	6.00	0.8742	21.18	-1.33	0.105
	7.00	0.9295	19.92	-1.30	0.112
	8.00	0.9435	19.63	-1.29	0.114
5×10^{-4} M	6.00	0.0821	22.57	-1.35	0.0099
	7.00	0.1081	17.13	-1.23	0.0130
	8.00	0.1195	15.50	-1.19	0.0144
Average values			20.26 ± 2.58	-1.30 ± 0.06	

^a pH at initial experimental condition of impregnation (± 0.01).^b Adsorbed amounts of malonic acid calculated as $\Gamma_{\text{AcMal}} = [\text{AcMal}]_{\text{ads}} V/mS$, where $V = 50.0$ ml, $S = 2.7$ m²/g, and $m = 5.0$ g.^c Relative amounts of adsorption according to $K_{\text{ads}} = [\text{AcMal}]/[\text{AcMal}]_{\text{ads}}$.^d $\text{p}K_{\text{ads}} = -\log K_{\text{ads}}$.^e Adsorbed molecules of malonic acid for the basic sites on surface calcite according to 5.0 site/m² [16].

bility in aqueous media is due to the dismutation processes and to the higher stability of other species in the chemical equilibrium.

The specific adsorption of malonic acid was obtained by $\Gamma_{\text{AcMal}} = [\text{AcMal}]_{\text{ads}} V/mS$ and represents the moles of malonic acid on the surface area of calcite. In Table 3 it is observed that the adsorbed amounts increase with the pH and the magnitude order is proportional to the respective initial concentration. The ratio between the initial concentration and adsorbed concentration of malonic acid given by $K_{\text{ads}} = [\text{AcMal}]/[\text{AcMal}]_{\text{ads}}$ shows quite similar values at any concentration and pH. In Fig. 4 the highest K_{ads} values implicate the smallest amount of adsorbate. K_{ads} can be associated with a global chemical equilibrium of the adsorption of malonic acid in the surface reaction $[\text{AcMal}]_{\text{ads}} \rightarrow [\text{AcMal}]$. Under this criterion, K_{ads} should be constant and it does not depend on the concentration or pH.

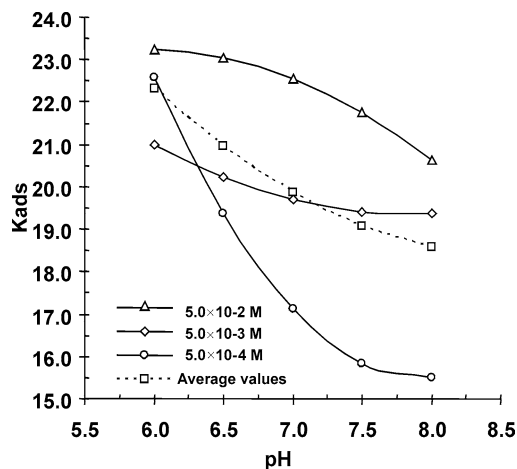


Fig. 4. Relative amounts of malonic acid adsorbed at 298 K. The discontinuous line shows the average tendency of K_{ads} as a function of pH.

3.5. Raman spectroscopy

We observed that when the effective adsorption of malonate ion on calcite occurs, the Raman vibrational modes reported in Table 4 are affected by the surface molecules. This can be seen in Figs. 5 and 6, where the 282.9 cm⁻¹ and 714.7 cm⁻¹ Raman peaks shift of calcite impregnated with a solution of malonic acid at pH 6.0 appear, respectively. For samples at pH 7.0 and pH 8.0, the Raman spectra

Table 4

Vibrational active modes in Raman spectroscopy for calcite (cm⁻¹)

Mode	Symmetry	Theoretical shift [38]	Experimental shift
ν_1	A _g	1088	1089.2
ν_4	E _g	714	714.7
ν_{13}	E _g	283	282.9

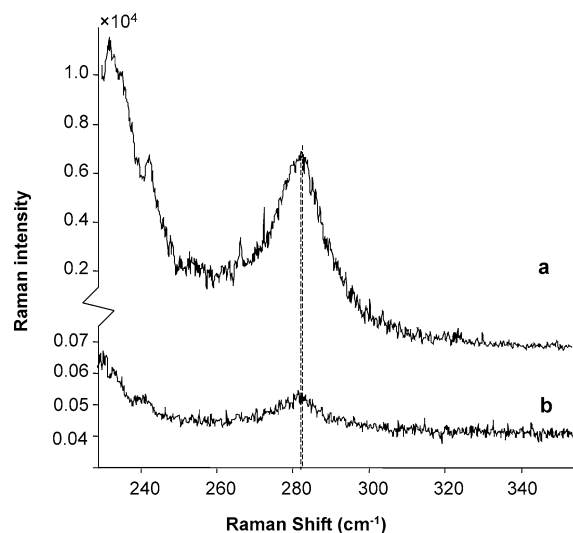


Fig. 5. Typical vibrational shift at 282.9 cm⁻¹ of Raman spectroscopy for calcite samples: (a) pure calcite and (b) calcite impregnated with malonic acid solution at 5.0×10^{-4} M and pH 6.0.

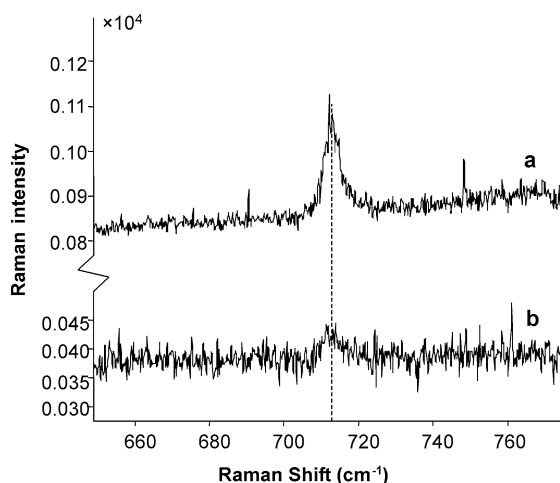


Fig. 6. Typical vibrational shift at 714.7 cm^{-1} of Raman spectroscopy for calcite samples: (a) pure calcite and (b) calcite impregnated with malonic acid solution at $5.0 \times 10^{-4} \text{ M}$ and pH 6.0.

were similar: the Raman intensity decreases dramatically compared to pure calcite, as can be noticed in Figs. 5b and 6b. In addition, we found that the band at 1089.2 cm^{-1} diminished in intensity with increasing concentration, as appears in Fig. 7. These differences suggest an increase of the amount of adsorbate on calcite due to the diminution of the induced polarizability of calcite. To verify this, the measurements were performed repeatedly in the plane $(10|4)$ of a calcite monocrystal impregnated with acid solutions. In a polycrystalline sample, there are no preferential planes, whereas deposition on the plane $(10|4)$ led to a refinement of the Raman spectra.

Fig. 8 shows the three characteristic Raman shifts in the refined spectra on the preferential cleavage of the calcite. In this case we found a strong coupling in the three bands (282.9 , 714.7 , and 1089.2 cm^{-1}). We assign these changes

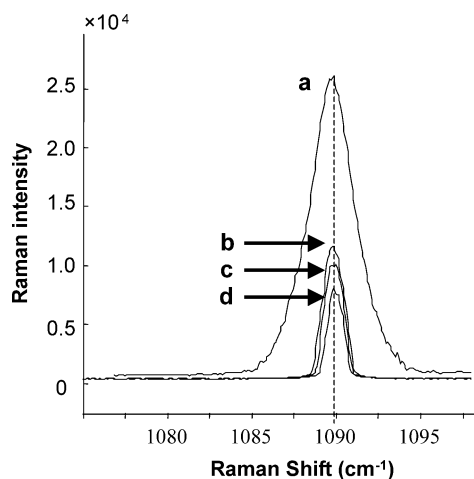


Fig. 7. Typical vibrational shift at 1089.2 cm^{-1} of Raman spectroscopy for calcite samples: (a) pure calcite, and calcite impregnated with malonic acid solutions at pH 6.0: (b) $5 \times 10^{-2} \text{ M}$, (c) $5 \times 10^{-3} \text{ M}$, and (d) $5 \times 10^{-4} \text{ M}$.

to a selective adsorption of malonate ion, corresponding to space-oriented vibrational bands.

3.6. SAXS

SAXS measurements give information on the homogeneity of the sample in the range of 10 to 300 \AA . The Kratky plots (see Fig. 9) show the variation of the pore shape. The specific tendency of carboxylate ions to adsorb in preferential planes modifies the average surface pore shape. As can be seen in Fig. 9a, pure calcite contains elliptical pores in its surface, whereas the shape turns out to be spherical when the sample is impregnated with a solution having pH 6.0. When the pH was 7.0 or 8.0 the pore shape changed to slits. According to these results, the pH strongly influences the pore shape. The change in the concentration did not produce sig-

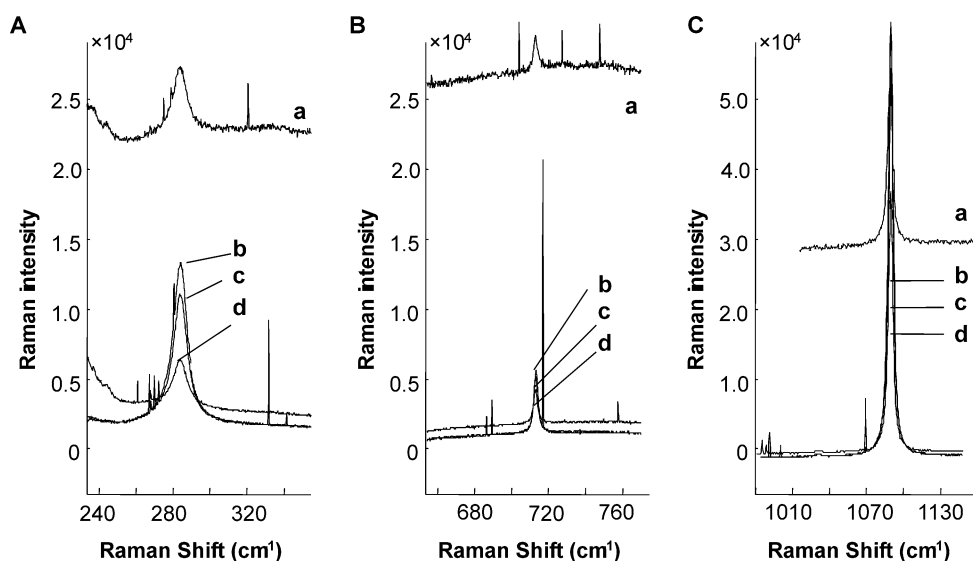


Fig. 8. Refined typical vibrational shift of Raman spectroscopy for calcite monocrystal samples in plane $(10|4)$. (A) 282.9 cm^{-1} ; (B) 714.7 cm^{-1} ; and (C) 1089.2 cm^{-1} . (a) Calcite, (b) calcite impregnated samples with malonic acid at $5.0 \times 10^{-4} \text{ M}$ and pH 6.0.

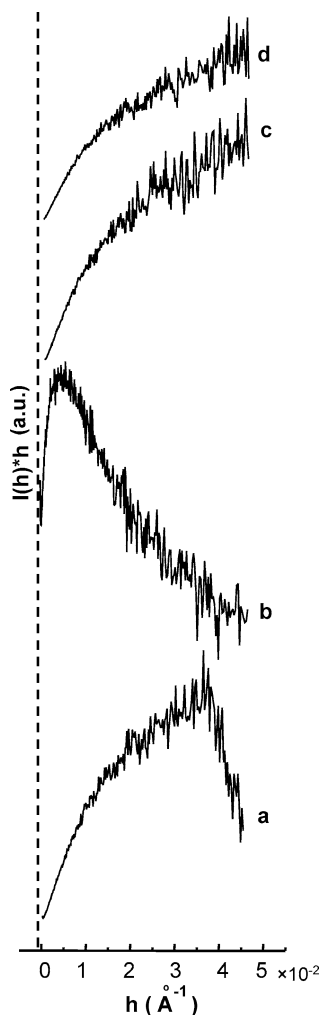


Fig. 9. Kratky plots obtained by SAXS in calcite impregnated with malonic acid solutions at 5.0×10^{-4} M: (a) calcite, (b) pH 6.0, (c) pH 7.0, and (d) pH 8.0.

nificant modifications of the pore shape, as spherical pores were detected in all cases (results not shown here). We suggest that the change of pore shape indicates that the malonate ions are deposited in layers or as clusters in the inner pore by adsorption in function to pH, resulting in a geometrical evolution of the final pore shape.

Fig. 10 shows the pore size distribution assuming the shapes determined by the Kratky plots. In all cases, a change in the pore size distribution is observed. The distribution is shifted to smaller pore sizes when the pH is increased. These changes in the pore size distributions suggest an apparent modification in the surface structure. Malonic acid diffuses homogeneously through calcite pores and maintains the original morphology of the surface at the highest concentrations, whereas at lower concentrations the filled pores are those where diffusivity is the highest. In Fig. 10 it can be seen that working at pH close to 8.0 (and correspondingly to PZC), a change in the pore size distribution occurs, and we consider that even layers are developed when the impregnation is carried out at a pH close to IP (pH 6.45).

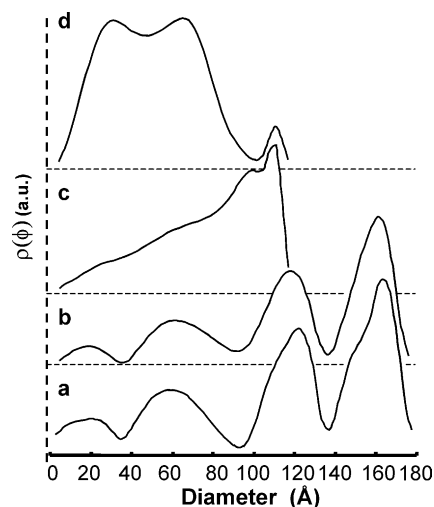


Fig. 10. Pore size distribution obtained by SAXS in calcite impregnated with malonic acid solutions at 5.0×10^{-4} M: (a) calcite, (b) pH 6.0, (c) pH 7.0, and (d) pH 8.0.

The electronic density functions show fluctuations at different pH (Fig. 11). This indicates the presence of dense surface layers deposited on top of the calcite surface that can be attributed to the adsorptive molecules, in correspondence with the pore size distribution. The packing of molecules in the inner pores changes the pore shape as well as the size.

4. Discussion

The adsorption of the malonate ion on calcite has been reported in the past [21–24], showing that there is a high affinity with the calcium ion. Based on the results obtained in this work, the malonate ions can be considered potential-determining ions and change the calcite surface charge. Gefroy et al. proposed an adsorption constant for malonic acid, $pK_{\text{ads}} = 1.4$ [24], defined by chemical equilibrium in aqueous complexation and surface speciation, but they did not define which species are involved in the adsorption (mono- or totally dissociated). In this work we obtained an average value quite close, $pK_{\text{ads}} = -1.30 \pm 0.06$ (see Table 3), where the minus sign appears due to the direction of chemical equilibrium referred to. According to these results, there is an approximately constant relationship between the initial concentration and the adsorbed amount.

Considering that the number of basic sites is 5.0 site/m² for polycrystalline calcite [16], it is observed (see Table 3) that the adequate concentration to reach a total surface coverage is 5.0×10^{-2} M, and the coverage diminishes at lower concentrations.

The proximity of the experimental pH values to IP and PZC has an influence in the final equilibrium of adsorption. In the impregnation, the PZC determines the final surface charge, where small values which are adequate to the aim of the present work; however, after washing, the IP determines the residual malonate amount on the surface. This is

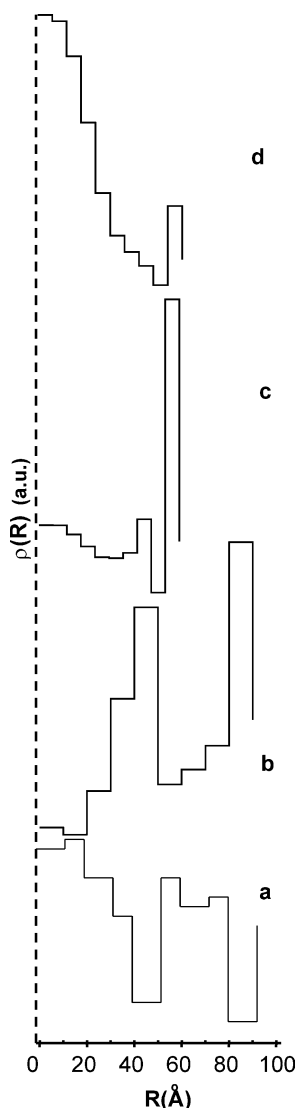


Fig. 11. Average electronic density functions obtained by SAXS in calcite impregnated with malonic acid solutions at 5.0×10^{-4} M: (a) calcite, (b) pH 6.0, (c) pH 7.0, and (d) pH 8.0.

explained by the electroneutrality (near PZC) and null electrophoretic mobility (near IP) as stability condition for the remains of the adsorbate on the surface; in the case of the impregnation the first condition predominates, and for the washing, the second condition.

Malonic acid is a highly polar compound and its polarizability in aqueous solutions strongly depends on the concentration. At high concentrations, it presents strong dipole–dipole interactions with the solvent and the polarizability is high. The adsorption of malonate ions modified the induced polarizability of the calcite surface as detected by Raman spectra (Figs. 5–8), as all the impregnated samples showed a reduction in the Raman intensity peaks. It was possible to establish the influence of the concentration of malonate ion only in the preferential vibrational mode (Raman shift 1089.2 cm^{-1}); it is possible to distinguish the difference between conditions.

Diffusion of the malonate ions also is a function of the concentration and it is related to the ion mobility in aqueous media (conductance), and, in a porous medium, it is also a function of the pore radii. According to the results, the ions diffused better in large pores and at lower concentrations. Regarding the pH dependence (Fig. 10), the approximation to the PZC favored the adsorption, as it was mentioned previously. The apparent change in the pore shape is related to the amount of malonate ion and the adsorption capacity in each experimental condition.

Based in the results presented in this paper, the adsorption depends on diffusional phenomena. Working at pH values close to IP ensures to cover the surface without occupying all the basic sites and the pore shape does not exhibit significant changes, and the distribution of the adsorbate in the surface is consistent with an equilibrium characterized by zero electrokinetic mobility. Working at a pH value close to PZC ensures coverage of only the largest pores or filling the highest pores first, and then smaller ones, to compensate for the surface charge of the cavities with adsorbate charge until a zero charge value is reached. The pore size distribution is then modified towards pores of intermediate size and also towards small pore sizes, and the pore shape changes according to specific molecular packing mechanisms.

The extreme change in the pore shape led the slit pore shape in condition of complete adsorption, whereas elliptical is the original pore shape of the calcite, and the spherical shape was the intermediate result.

5. Conclusions

The adsorption of malonate ion on a calcite surface was accomplished. According to the results, pH is the most important variable in the effective surface adsorption.

The optimum impregnation of malonate ion was accomplished at a pH close to the PZC (pH ~ 8.2). In impregnations performed at pH values closer to the IP (pH ~ 6.2), the adsorbate remained bonded to the surface after washing. Higher concentrations led to better coverage of the surface.

The adsorption of malonate decreased the polarizability of the calcite surface and this was detected by Raman spectroscopy. The adsorption of carboxylate ions occurs preferentially on the cleavage plane (10|4) in a calcite monocrystal. The adsorption on this sample refined the Raman spectra, showing an intensity coupled to the three characteristic vibrational bands.

The pore size distribution is related to diffusivity of malonate ion. At higher concentrations malonate ions produced homogeneous layers on the surface. The covering and packing of malonate ion changed the apparent pore shape and surface electronic density. The adsorption generates a potential that can be effective in protecting the surfaces. This can be used as an effective approach in preventing damage on cultural heritage materials of limestone and marble.

Acknowledgments

M.F. Salinas-Nolasco acknowledges CONACYT-México for a fellowship. The authors acknowledge Dr. E. Haro-Poniatowski and Dr. M.A. Camacho-López for performing the Raman analysis.

References

- [1] H.A. Lowenstan, *Science* 211 (1981) 1138.
- [2] L. Addadi, N. Berkovitch-Yellin, N. Domb, E. Gati, M. Lahav, L. Leiserowitz, *Nature* 296 (1982) 21.
- [3] S. Mann, *Nature* 332 (1988) 119.
- [4] S. Mann, *Nature* 365 (1993) 499.
- [5] S. Mann, D.D. Archibald, J.M. Didymus, T. Douglas, B.R. Heywood, F.C. Meldrum, N.J. Reeves, *Science* 261 (1993) 1286.
- [6] K.L. Nagy, R.T. Cygan, C.S. Scotto, C.J. Brinker, C.S. Ashley, in: *Mater. Res. Soc. Symp. Proc.*, vol. 462, 1997, p. 301.
- [7] G. Wheeler, J. Méndez-Vivar, S. Flemming, *J. Sol–Gel Sci. Technol.* 26 (2003) 1233.
- [8] Y. Kitano, D.W. Hood, *Geochim. Cosmochim. Acta* 29 (1965) 29.
- [9] A.R. Hoch, M.M. Reddy, G.R. Aiken, *Geochim. Cosmochim. Acta* 64 (1999) 61.
- [10] J.S. Duca, A.J. Hopfinger, *Chem. Mater.* 12 (2000) 3821.
- [11] N.H. Leeuw, S.C. Parker, *J. Phys. Chem. B* 102 (1998) 2914.
- [12] H. Ruuska, P. Hirva, T.A. Pakkanen, *J. Phys. Chem. B* 103 (1999) 6734.
- [13] S. Hwang, M. Blanco, W.A. Goddard III, *J. Phys. Chem. B* 105 (2001) 10,746.
- [14] Ö. Nilsson, J. Sternbeck, *Geochim. Cosmochim. Acta* 63 (1999) 217.
- [15] O.S. Pokrovsky, J.A. Mielczarski, O. Barres, J. Schott, *Langmuir* 16 (2000) 2677.
- [16] P. Van Cappellen, L. Charlet, W. Stumm, P. Wersin, *Geochim. Cosmochim. Acta* 57 (1993) 3505.
- [17] P. Fenter, P. Geissbühler, E. DiMasi, G. Srajer, L.B. Sorensen, N.C. Sturchio, *Geochim. Cosmochim. Acta* 64 (2000) 1221.
- [18] R.G. Compton, K.L. Pritchard, P.R. Unwin, G. Grigg, P. Silvester, M. Lees, W.A. House, *J. Chem. Soc. Faraday Trans.* 85 (1989) 4335.
- [19] A.J. Barwise, R.G. Compton, P.R. Unwin, *J. Chem. Soc. Faraday Trans.* 86 (1990) 137.
- [20] P.R. Unwin, R.G. Compton, *J. Chem. Soc. Faraday Trans.* 86 (1990) 1517.
- [21] S. Mann, J.M. Didymus, N.P. Sanderson, B.R. Heywood, E.J.A. Sampoer, *J. Chem. Soc. Faraday Trans.* 86 (1990) 1873.
- [22] N. Wada, K. Kanamura, T. Umegaki, *J. Colloid Interface Sci.* 233 (2001) 65.
- [23] M.M. Reddy, A.R. Hoch, *J. Colloid Interface Sci.* 235 (2001) 365.
- [24] C. Geffroy, A. Foissy, J. Persello, B. Cabanet, *J. Colloid Interface Sci.* 211 (1999) 45.
- [25] O. Glatter, *J. Appl. Crystallogr.* 14 (1981) 101.
- [26] O. Glatter, *J. Appl. Crystallogr.* 21 (1988) 886.
- [27] O. Glatter, K. Gruber, *J. Appl. Crystallogr.* 26 (1993) 512.
- [28] O. Glatter, B. Hainisch, *J. Appl. Crystallogr.* 17 (1984) 435.
- [29] M. Kataoka, Y. Hagihara, K. Mihara, Y. Goto, *J. Mol. Biol.* 229 (1993) 591.
- [30] D.L. Graf, *Am. Mineral.* 46 (1961) 1283.
- [31] S.L.S. Stipp, *Geochim. Cosmochim. Acta* 63 (1999) 3121.
- [32] G.W. Akin, J.V. Lagerwerff, *Geochim. Cosmochim. Acta* 29 (1965) 343.
- [33] L. Charlet, P. Wersin, W. Stumm, *Geochim. Cosmochim. Acta* 54 (1990) 2329.
- [34] J.W. Morse, *Mar. Chem.* 20 (1986) 91.
- [35] D.W. Thompson, P.G. Pownall, *J. Colloid Interface Sci.* 131 (1989) 74.
- [36] S.G. Bratsch, *J. Chem. Educ.* 62 (1985) 101.
- [37] M. Randic, *J. Math. Chem.* 7 (1991) 155.
- [38] K. Nakamoto, *Infrared and Raman Spectra of Inorganic and Coordination Compounds. Part A: Theory and Applications in Inorganic Chemistry*, Wiley–Interscience, New York, 1997, pp. 124–140.